

Casualty and Fatality Rates of Massive Extinction After Asteroid Impact with Earth

Guillermo Ortega⁽¹⁾, Tommaso Sgobba⁽²⁾, Irene Huertas⁽³⁾,
Francesco Cremaschi⁽⁴⁾, Chris Laurel⁽⁵⁾

(1) European Space Agency, Keplerlaan 1, AG2200, Noordwijk, The Netherlands
Guillermo.Ortega@esa.int

(2) European Space Agency, Keplerlaan 1, AG2200, Noordwijk, The Netherlands
Tommaso.Sgobba@esa.int

(3) European Space Agency, Keplerlaan 1, AG2200, Noordwijk, The Netherlands
Irene.Huertas@esa.int

(4) Astos Solutions GmbH, Grund 1, 78089, Unterkirnach,, Germany
Francesco.Cremaschi@astos.de

(5) Periapsis Visual Software, 626 Randolph Pl, WA 98122 Seattle, United States
CLaurel@gmail.com

INTRODUCTION

This paper focuses on a detailed mathematical model that is able to calculate casualty and fatality rates after the impact of an asteroid with Earth. The mathematical model has been programmed in a software tool and the corresponding casualty and fatality curves have been computed.

The mathematical model takes into account the impact of an asteroid and the subsequent destruction of life and properties. The model divides the destruction process in consecutive segments starting from the instant of the impact and allows to forecast the levels of casualties and fatalities until reaching massive extinction. This mathematical model has been validated with previous recorded catastrophes and represents a step ahead in the protection of civilians and their habitats dividing the population into sheltered and un-sheltered. The model uses the most accurate world population data base, the latest model of the Earth atmosphere, and high accuracy re-entry trajectories for the threatening asteroid.

PURPOSE, DEFINITIONS, AND PROCESSES

The purpose of the study was to conduct a parametric analysis to calculate fatality curves as a function of the size of an asteroid impact with Earth, its inner composition, its speed, its flight path angle at Earth entry, and its primary impact location on our planet. This massive amount of data shows revealing conclusions that will be shown in this paper.

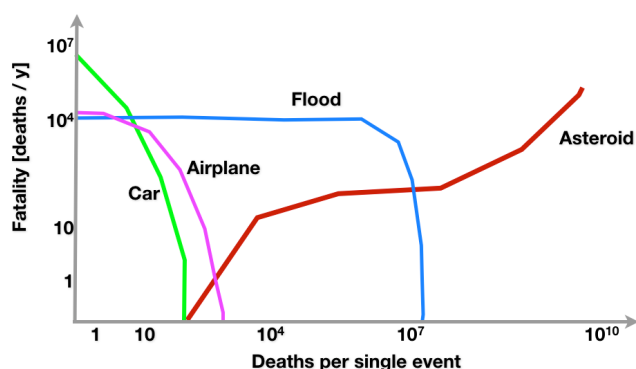


Figure 1. Deaths versus fatality curve and polyhedron model of the asteroid "Eros"

The paper is complemented by a presentation handout (available on demand) that contains the display of a realistic set of videos made from the simulations of one of the most damaging impacts of the asteroid simulation sets. The videos show the propagation of the extinction wave for the most dramatic case.

It has to be pointed out that no registry of anybody ever been killed by an asteroid impact has been made till date. Therefore, this research acknowledges that the threat of the case of the asteroid or comet hitting Earth is small in comparison with other catastrophes. Figure 1 shows the death per single event versus the corresponding fatality expressed in deaths per year. For example, the graph shows that fatality rates in all recorded automobile history reaches the sum of all accidents in all cars involved. The same for the airplane accidents, floods, etc. In a given year, the probability to be killed in a car accident is higher than the probability to die in an airplane accident or in a flood. And much higher than the probability to die due to an asteroid impact with Earth. However, it is recognized that a medium size asteroid impact with Earth is more lethal than anything Earth or humans are capable of producing on the scale of massive destruction. The current study also provides awareness of the Earth's fragility and establishes grounds for studying the risk management to population in the following terms: quantification of the magnitude of the risk, the identification of risk contributions, the study of damage to life and properties, and open discussion about the uncertainties in the mathematical model.

The following definitions are used in this paper:

- **Earth catastrophic event:** more than 10.000 people killed at the same time.
- **Property damage:** damage to fixed and non-fixed property owned by a person or group of persons.
- **Casualty:** a person suffering small injury as the result of a catastrophic event.
- **Fatality:** a person suffering death or serious injury as the result of an accident associated with a catastrophic event.
- **Maximum Probable Loss (MPL):** the greatest Euro amount of loss for bodily injury or property damage that is reasonably expected to result from a catastrophic event.

ASTEROID THREAT

The table 1 shows a catalogue of asteroid threats as a function of the diameter of an asteroid impacting the Earth. The damages go from local destruction to the total planetary collapse. The minimum impact velocity on Earth is 11 km/s. The typical impact velocities are more than 15 km/s for asteroids and more than 50 km/s for comets. The maximum Earth impact velocity for objects orbiting the sun is 72 km/s.

Diameter [Km]	Kinetic energy at impact [MT]	Recurrence interval time of the same impact again [y]	Crater diameter [Km]	Crater depth [Km]	Earthquake magnitude [Richter]	Severity
0.01	0.06	6.38	0.3	0.4	3.8	Local destruction
0.1	75.16	1,583.60	1.9	0.6	5.9	Local catastrophe
1	7.52E+04	346,454.27	11.4	1.0	7.9	Regional catastrophe
5	9.39E+06	1.50E+07	39.9	1.5	9.3	Global catastrophe
10	7.52E+07	7.58E+07	68.5	1.8	9.9	Massive extinction
100	7.52E+10	1.66E+10	412.9	3.0	11.9	Planetary collapse

Table 1. Asteroid threat catalogues as a function of the diameter

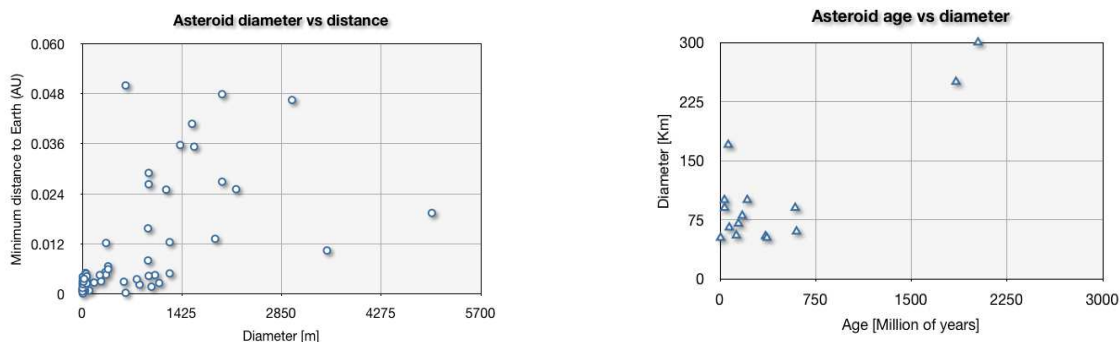


Figure 2. Asteroids versus diameter and versus age

To allow a comparison, the Hiroshima and Nagasaki atomic bombs were 20 KiloTones (KT) of energy. The biggest ever recorded Earthquake magnitude has been 9.5. The K-T boundary extinction (Cretaceous–Tertiary extinction event) energy was about $1E+7$ MT. And the energy to boil all Earth oceans is about $2E+9$ MT. Figure 2 shows two graphs of the known asteroids versus their know diameters and their age. Bigger asteroids are far away and are older that smaller nearer objects in average.

SETTING UP THE SIMULATION SCENARIO

The simulation work reported in this paper has been segmented into phases as follows:

- Phase 1: represents the travel in space of the astroid. The asteroid travels in space with the simulation starting at around GEO altitude (i.e. 42000 Km approximately).
- Phase 2: is the phase when the asteroid is entering the Earth atmosphere: the asteroid enters Earth atmosphere at 120 Km.
- Phase 3: is the impact with Earth at the impact point and flight of ejecta around
- Phase 4: represents the shock wave and how it propagates on Earth from the impact point and in the direction of the azimuth foreseen.

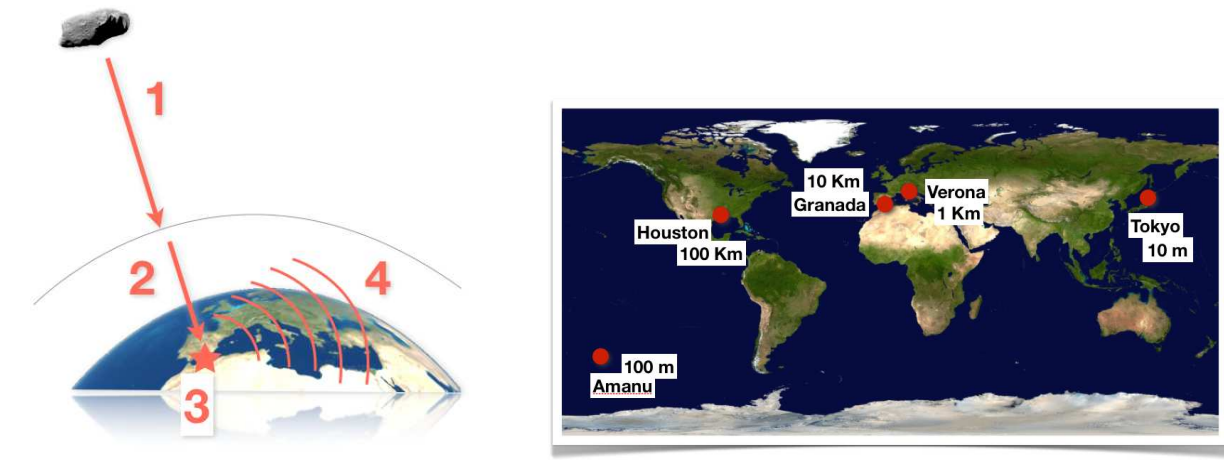


Figure 3. Simulation scenario segmented in phases and targeted impact points with asteroid diameters

The figure 3 shows an schematic view of the simulation segmented into 4 phases. To these phases the study also adds a phase called phase 4+1 that shows the aftermath long-term effects after the shock wave has propagated. The figure 4 also shows the targeted impacts with their corresponding asteroid diameter sizes. The impact points have been chosen as to reflects dispersed areas of the Earth. The sizes of the asteroid range from 10 meters to 100 Kilometers. The impacts points are Amanu, Houston, Verona, Granada, and Tokyo.

ATV RE-ENTRY AS A RISK CALCULATION EXAMPLE

The controlled re-entry of ATV created a concern among ESA and CNES officials in what respect to casualty and fatality figures. In September 2008 ESA initiated a series of detailed studies to accurately compute these figures and the corresponding ground risk foot prints. The results obtained by the Technical Directorate of ESA used state of the art mathematical models that have been independently verified and validated. ATV broke into approximately 600 main fragments and many other much smaller.

The Automated Transfer Vehicle was designed to end its mission by a destructive re-entry using the earth atmosphere. The de-orbitation scenario started with the departure of the vehicle from the ISS followed by a drift period to phase with the targeted impact area. Once this phasing was finished ATV performed two de-orbitation boosts which caused it to enter the atmosphere and started fragmentation by aerodynamic and thermal loads. ATV Jules Verne re-entered Earth on September 29th 2008 ending a very successful first mission for ESA and its partners. The first de-orbitation burn

(see figure 4) changed the ATV orbit from circular to highly elliptical while the second one targeted Zero-altitude periapsis and subsequent collision with Earth.

ATV was composed of two main parts: the spacecraft subassembly, and the integrated cargo carrier. ATV used four solar arrays skewed about 45 deg for power and communicated via a S-band antenna mast mounted (see figure 4). The materials list of which the subsystems of Jules Verne are made represent about 100 different collection types: from Titanium to Aluminum, from Beryllium, to carbon fiber, etc. Figure 4 shows the sizes of ATV and its comparison with the size of the average human being. The total length is about 10 meters while the total diameter is about 4.5 meters.

To study ATV re-entry safety in depth, ESA and CNES constituted a task force in Spring 2007 with experts and engineers from both Agencies.

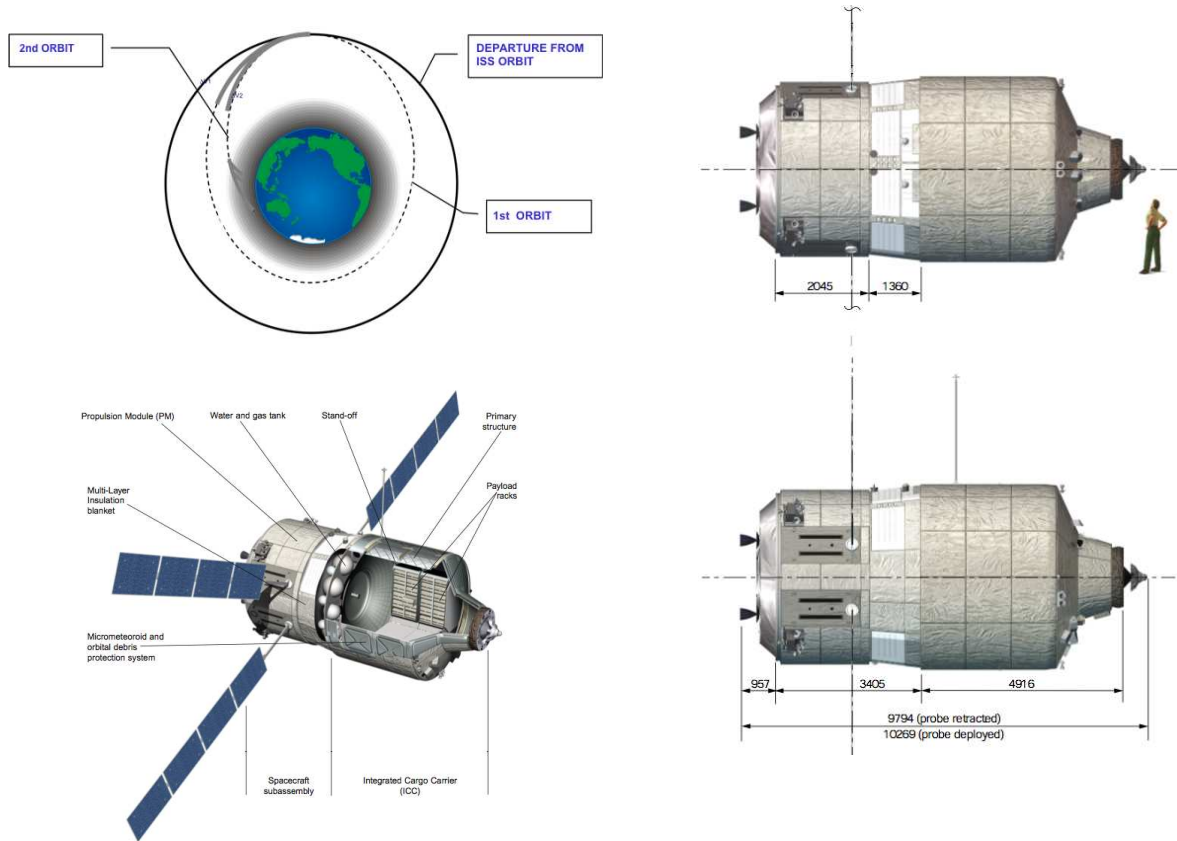


Figure 4. ATV re-entry strategy and model

The task force recommended to perform a detailed risk analysis for the re-entry phase of Jules Verne and the evaluation of the casualty and fatality probabilities versus the acceptable standards. The task force started to perform the analysis end of April 2007.

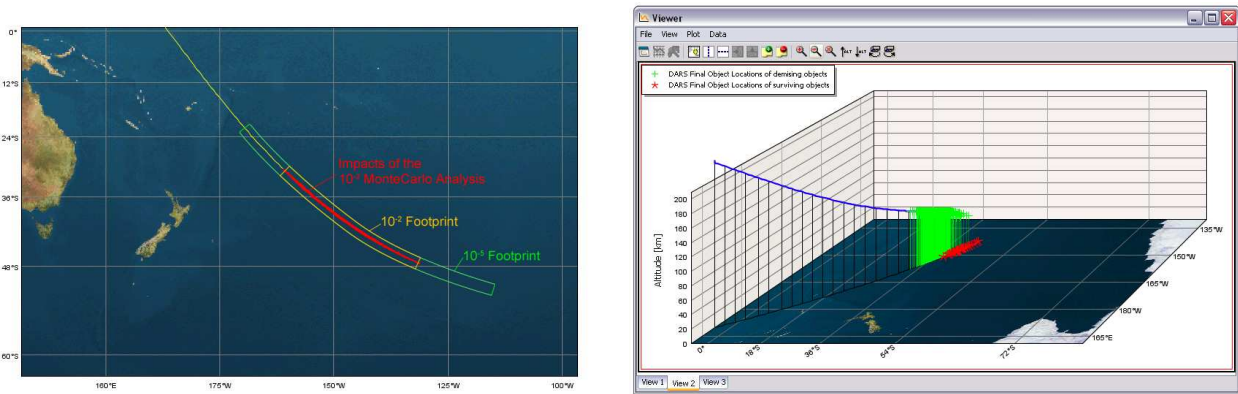


Figure 5. ATV re-entry risk analysis calculation

At this point in time, commanded by the ATV Re-entry Safety Panel and via ATV operations team, the Technical Directorate of ESA started to work in the risk analysis while the Operations Directorate team supported the Panel in an independent verification of the work of ESTEC. ESTEC assessed the final ATV disposal cargo list w.r.t. their contribution to the surviving fragments list in the case of an uncontrolled re-entry. And it computed several trajectory types with their corresponding casualty and fatality risks. All in total, ESTEC ran about 20 million of trajectories in two analysis phases. The trajectories varied six parameters: the duration of the last impulse burn, the level of the thrust, its angle, the density of the atmosphere, the altitude of the explosion, and the direction of the ejection of the fragments.

The present asteroid scenario study takes into account the ATV re-entry experience by re-using techniques and technologies from the former work in the ESA project.

ASTOS, THE AEROSPACE TRAJECTORY OPTIMIZATION SOFTWARE

The software tool used in the analysis and simulations reported in this paper is ASTOS.

Trajectory risk analysis tools are starting to become important assets to address the human casualty risk from any portions of the spacecraft or orbital stages that may survive atmospheric re-entry. These tools shall not only include the calculation of casualty area but also the casualty and fatality probabilities.

ASTOS software (see figure 6) is a simulation and optimization environment to compute optimal trajectories for a variety of complex multi-phase optimal control problems. It consists of fast and powerful optimization programs, PROMIS, CAMTOS, SOCS and TROPIC, that handle large and highly discretized problems, a user interface with multiple plot capability, and GISMO, an integrated graphical iteration monitor to review the optimization process and plot the state and control histories at intermediate steps during the optimization. Since 1995, ASTOS is being developed in collaboration with the Technical Directorate of the European Space Agency at ESTEC. Since 2005, three modules were added inside ASTOS: DARS (Debris Analysis for Re-entering Spacecraft) that calculates the vehicle re-entry considering break-up and demise [7], and DIA (Debris Impact Analysis) [8] that calculates the impact based on ballistic coefficients. On top the risk probabilities of casualties and fatalities can be calculated with RAM (Risk Analysis Module).

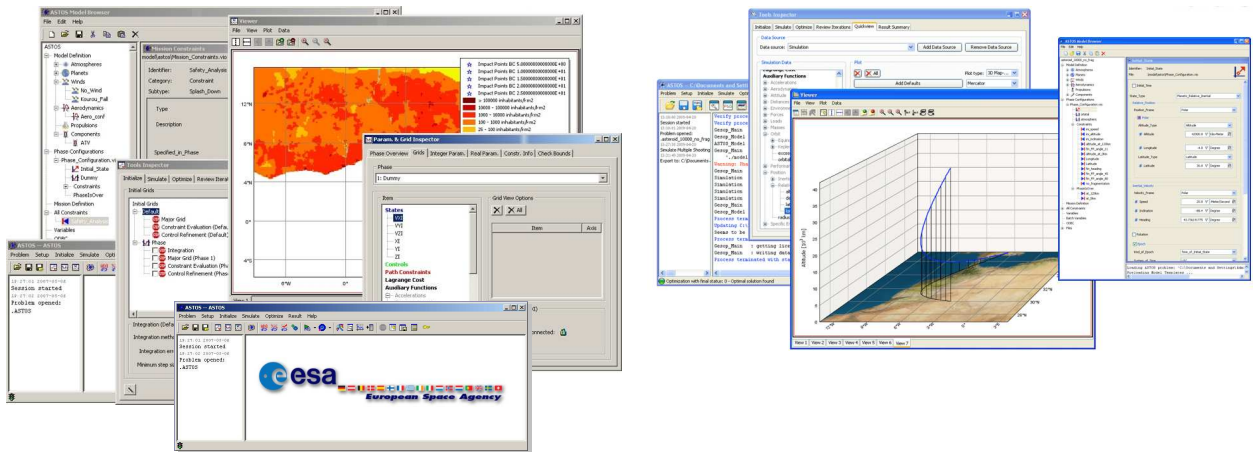


Figure 6. ASTOS screenshots, including GPWv3 population overlays

DARS, as a deterministic tool, considers not only a vehicle break-up, but also melting of the fragments, taking diverse materials and shapes into account. DIA is based on ballistic coefficients and allows safety analysis in combination with additional impulses during the break-up already in early project phases. Both, DIA and DARS can be combined with stochastic methods for extensive calculations of variations. RAM calculates the casualty cross-section (A_c) of a re-entry object. ASTOS can generate plots in 2D and 3D. The inputs to this process are the scenario, vehicle, orbital dynamics, and the outputs are trajectories, foot-prints, dispersion ellipsoids, reports, etc. ASTOS uses the population data from the Gridded Population of the World Version 3 (GPWv3). GPWv3 depicts the distribution of human population across the globe. It is the most detailed version of GPW to date with more than three times the amount of data as version 2, and includes population estimates to 2015.

PHASE 1: ASTEROID INTERPLANETARY TRIP

The phase 1 of the simulation study represents the travel in space of the asteroid. The simulation starts at around GEO altitude (i.e. 42000 Km approximately). The asteroid flight speed at that altitude is between 20 to 30 Km/s. The simulation date chosen is December 21st, 2012.



Figure 7. Video of the asteroid flight for phase 1

The figure 7 shows a screenshot of the video made from the asteroid trajectory for phase 1. The average density of the simulated asteroid ranges from 3000 to 4000 Kg/m³. Its composition is a mixture of olivine and pyroxene with the following ingredients and their corresponding percentages: Mg (10.98%), Fe (12.33%), Si (35.67%), O (14.05%), Ca (19.54%), Al (4.71%), Na (0.81%), K (0.14%), Ti (0.58%), Mn (0.23 %), H (0.96%).

Asteroid features							Impact consequences										
Material density [kg/m ³]	Diameter [Km]	Surface [m ²]	Volume [m ³]	Mass [Kg]	Flight path velocity [Km/s]	Flight path angle [deg]	Kinetic energy at impact [J]	Kinetic energy at impact [MT]	Recurrence interval time of the same impact again [y]	Crater diameter [Km]	Crater depth [Km]	Earthquake magnitude [Richter]	Initial ground speed of ejecta [m/s]	Ejecta time to reach ground [s]	Maximum height of ejecta [Km]	Extinction	
3000	0.01	7.9E+01	5.2E+02	1.6E+06	10	45	7E+13	0.02	2.16	0.2	0.3	3.4	7,849.1	0.1	0.00	No	
3000	0.1	7.9E+03	5.2E+05	1.6E+09	10	45	8E+16	18.79	537.08	1.4	0.6	5.4	8,509.0	0.9	0.00	No	
3000	10	7.9E+07	2.1E+12	6.3E+15	10	45	8E+22	1.88E+07	25,706,273.22	50.5	1.6	9.5	4,254.5	86.8	36.94	YES	
3000	100	7.9E+09	2.1E+15	6.3E+18	10	45	8E+25	1.88E+10	5,623,919,805.50	304.4	2.8	11.5	4,254.5	868.3	3,694.07	YES	
3000	0.01	7.9E+01	2.1E+03	6.3E+06	20	45	3E+14	0.06	6.38	0.3	0.4	3.8	7,849.1	0.2	0.00	No	
3000	0.1	7.9E+03	2.1E+06	6.3E+09	20	45	3E+17	75.16	1,583.60	1.9	0.6	5.9	8,509.0	1.7	0.01	No	
3000	10	7.9E+07	2.1E+12	6.3E+15	20	45	3E+23	7.52E+07	75,795,934.61	68.5	1.8	9.9	8,509.0	173.7	147.76	YES	
3000	100	7.9E+09	2.1E+15	6.3E+18	20	45	3E+26	7.52E+10	16,582,343,699.51	412.9	3.0	11.9	8,509.0	1,736.5	14,776.26	YES	
3000	0.01	7.9E+01	2.1E+03	6.3E+06	30	45	6E+14	0.14	12.01	0.4	0.4	4.0	11,773.7	0.3	0.00	No	
3000	0.1	7.9E+03	2.1E+06	6.3E+09	30	45	7E+17	169.10	2,980.91	2.3	0.6	6.1	12,763.6	2.6	0.03	No	
3000	10	7.9E+07	2.1E+12	6.3E+15	30	45	7E+23	1.69E+08	142,675,129.88	81.9	1.9	10.1	12,763.6	260.5	332.47	YES	
3000	100	7.9E+09	2.1E+15	6.3E+18	30	45	7E+26	1.69E+11	31,213,917,385.17	493.5	3.2	12.1	12,763.6	2,604.8	33,246.59	YES	

Table 2. Round of performed simulations and their main parameters

PHASE 2: ENTERING THE EARTH ATMOSPHERE

This phase simulates when the asteroid is entering the Earth atmosphere at 120 Km altitude. the study performed an entry parametric analysis of several diameter sizes asteroids, several flight path angles and flight path azimuths.

Based on the parametric analysis done, the mathematical model used is able to calculate the kinetic energy at impact (in Megatons and Jules), the recurrence interval time (i.e. the time between two consecutive impacts of the same energy), and the dimensions of the crater. The model provides as well the Earthquake magnitude produced, the speed of the eject, the time to reach ground, and its maximal altitude. For this phase, one of the main parameters has been the flight path velocity that has been varied between 10 km/s and 30 km/s. This parameter has a great influence on the energy dissipated at impact and the corresponding consequences. The flight path angle has been kept at 45 degrees, representing an average impact angle. Even if it is highly improbable that an asteroid of this dimension (e.g. 10km) will fragment in the atmosphere a fragmentation scenario has been simulated to show the power and flexibility of the tools and mathematical models involved.

PHASE 3: IMPACTING EARTH

This phase shows the impact with Earth at the impact point and the corresponding flight of ejecta around it (figure 8). In this phase, the study conducted a parametric analysis based on previous cases plus changing the impact velocity on Earth.



Figure 8. Screenshots of the videos made for the impact with Earth with and without fragmentation

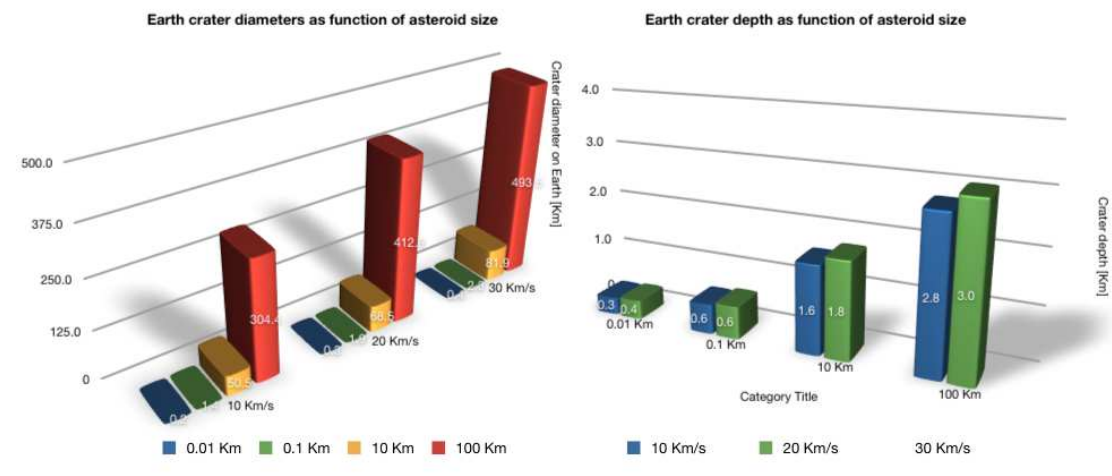


Figure 9. Craters diameters and depths as a function of impact speed and size

For this phase, the RAM module of ASTOS is used to calculate the casualty cross-section (A_c) of the asteroid. A_c is computed using the the cross-section of all asteroid fragments and an average projected cross section of a human body. The probability of casualty is determined using this casualty cross-section, the impact probability, and a population density distribution map. The risk to the population on-ground is determined by integrating the probability over a terrain area with underlying population density. To calculate the fatality index by a given piece of fragment with a given kinetic energy, it is necessary to multiply the probability of impact by the fatality index.

The function found is an halved gaussian shaped curve that ends in an exponential (see figure 10). The higher the value of the damage, the lower the probability that the damage actually occurs. The MPL figures are given in figure 11.

One of the cases computed is the un-fragmented impact in Granada. In this case, the energy released at impact is 7.5×10^7 MT (MegaTons of TNT). The Earthquake produced has a of magnitude of 9.9. The crater diameter is 69 km and has a depth of 1.8 km. The average ejecta thickness is 14.8 m. The mean fragment diameter is 5.43 cm. And the area of devastation at impact points is 107 Km^2 . For this Granada impact case, the wood frame and multistory wall-bearing buildings will collapse. The interior partitions of wood frame buildings will be blown down. Roofs will be severely damaged. Multistory steel-framed office-type buildings will suffer extreme frame distortion, mostly with incipient collapse. Highway truss and girder bridges will collapse. Cars and trucks will be overturned and displaced. Glass windows will shatter. And up to 90 % will be blown down, and those left standing will be stripped of branches and leaves.

Diameter [Km]	Kinetic energy at impact [MT]	Casualties	Fatalities	City
0.01	0.06	1.60	1.60	Tokyo
0.1	75.16	260.00	260.00	Amanu
1	7.52E+04	1,245.00	1,245.00	Verona
10	7.52E+07	2.38E+05	2.38E+05	Granada
100	7.52E+10	2.21E+07	2.21E+07	Houston

$$y = 470.12e^{0.1135x}$$

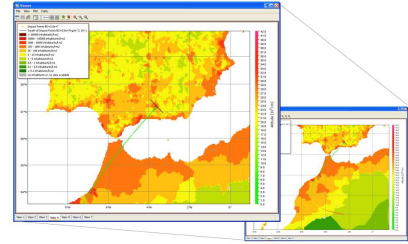
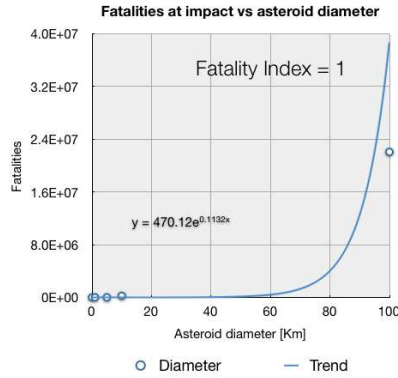


Figure 10. Casualties and fatalities per impact point with points and trend

Figure to Calculate	Definition	Comments / Formulas	Values
N_c	Number of Casualties	-	2.38E+05
N_F	Number of Fatalities	-	2.38E+05
MPL_F	MPL for third-party fatalities	$MPL_F = N_F * I_f$	€1,790,000,000
MPL_C	MPL for third-party casualties	$MPL_C = N_c * I_c$	€1,790,000,000
MPL_{LoP}	MPL for third-party loss of property	$MPL_{LoP} = 0.5 * N_c * I_c$	€895,000,000
MPL_{LoUP}	MPL for third-party loss of use of property	$MPL_{LoUP} = N_c * GDP$	€168,260,000
MPL_{ED}	MPL for third-party environmental damage	$MPL_{LoP} = S * I_{ED}$	€13,400,000
Total MPL			€4,656,660,000

Figure 11. MPL figures for the Granada impact case.

The fatality number computed takes into account only the people killed by a direct asteroid hit.

PHASE 4: PROPAGATION OF THE SHOCK WAVE

The phase four represents the shock wave and how it propagates on Earth from the impact point and in the direction of the azimuth foreseen. The simulation shows that the energy due to the impact will cause a distortion in the air. This distortion travels in the form of a shock wave, at a velocity greater than the speed of sound in air (hypersonic).

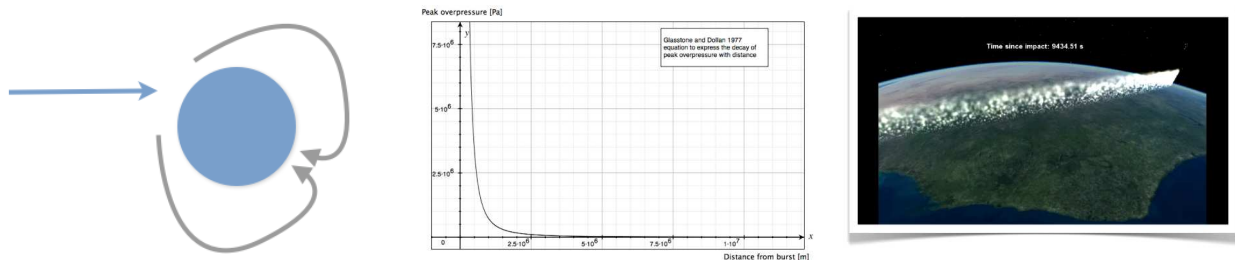


Figure 12 Shock wave propagation mathematical model and screenshot of the video simulating it

The wave eventually decays into a sound wave traveling at sonic speed (300 m/s). The mathematical model used predicts that the air blast will be generated approximately 1000 seconds after impact. The peak over-pressure will reach 8×10^6 Pa (80 bar). The maximum wind velocity will become 1310 m/s (hypersonic regime). During the propagation of the shock wave, sound intensity will reach 129 dB.

PHASE 4+1: EFFECTS AFTER SHOCK WAVE

The last phase of the simulation has been named in this study as phase 4+1. In this phase, the effects after the shock wave have been simulated. They are divided into two main sub-phases catalogued as post shock wave and long term effects.

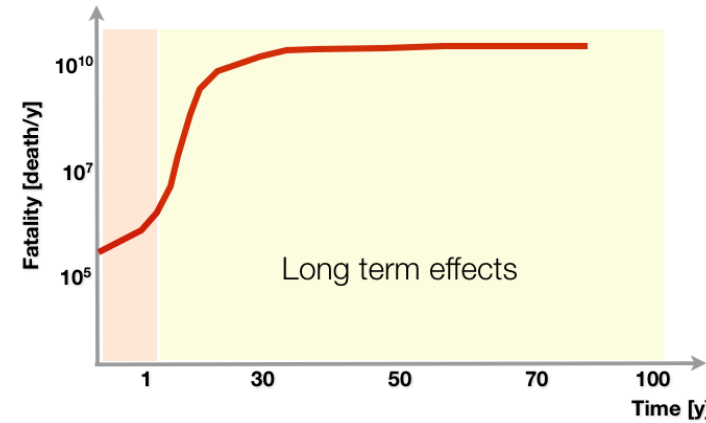


Figure 13 Fatality curve vs time after shock wave

The figure 13 shows the fatality curve vs time in this phase. During the first sub-phase (post shock wave), dust, melt droplets, and gas species generated during the impact event are ejected out of the Earth's atmosphere and dispersed all over the globe. Also during this sub-phase, tsunami cresting will reach 100 m altitude above sea level flooding 20 Km of coastline. During the second sub-phase (long-term effects), nitrous oxide will destroy the ozone layer causing more fatalities. At this stage, vision will not be possible and plants and forest will die.

CONCLUSIONS

The Technical Directorate of ESA has built a mathematical model of an asteroid impacting with Earth. Using this model, the purpose of the study was to conduct a parametric analysis to calculate fatality curves as a function of the size of an asteroid impact with Earth, its inner composition, its speed, its flight path angle at Earth entry, and its primary impact location on our planet.

Asteroid impacts represent hazard of low probability but high consequences. Risk of impact is substantially larger than one-in-a-million lifetime risk of death use in ESA terms when conducting the launch or re-entry of space vehicles.

The study performed in this work shows that asteroid impacts of the sizes proposed in this paper will kill billions of people and produce a massive extinction of species (endangering the survival of civilization).

While the role of governments is impact deflection, impact mitigation, and catastrophe management, the role of space agencies is limited to public awareness, threat detection, prediction, and risk analysis.

REFERENCES

[1] Andrea Milania, Steven R. Chesleya, Giovanni B. Valsecchi, "Asteroid close encounters with Earth: risk assessment", Planetary and Space Science 48 (2000) 945–954.

- [2] Steven N. War, Erik Asphaug, "Asteroid impact tsunami of 2880 March 16", *Geophysical Journal International* 2003, 153, F6–F10
- [3] Jack G. Hills, M. Patrick Goda. "Damage from Come-Asteroids Impacts with Earth". *Physica D* 133, 1999, 189-198.
- [4] Duncan Steel. "Distributions and moments of asteroid and comet impact speeds upon the Earth and Mars" *Pergamon Planet. Space Science*, Vol. 46, No. 5, 473-478, 1998 Elsevier Science Ltd
- [5] Curt Covey, Starley L. Thompson, Paul R. Weissman, Michael C. MacCracken. "Global Climatic Effects of Atmospheric Dust from an Asteroid or Comet Impact on Earth" *Global and Planetary Change* 9, 1994, 263-273
- [6] J.A.M. McDonnell, A.D. Griffiths, J.C. Zarnecki, D.J.Catling, S.F.Green, M.A.Fowler, N. ME.A.Taylor.. "Meteoroid and Debris Flux and Ejecta Models". ESA Contractor Report, Unispace Kent (UK), December 1998.
- [7] S. Weikert, F. Cremaschi, G. Ortega. "Probabilistic and Deterministic Re-entry Risk Mitigation Using ASTOS", Proceedings of the 3rd IAASS Conference, Building A Safer Space Together, Rome, Italy, 21-23 October 2008
- [8] A. Wiegand. "ASTOS Software User Manual, Version 6.0", ASTOS Solutions GmbH 2006.
- [9] T. Saitoa, K. Kaihob, A. Abec, M. Katayamac, K. Takayamad. "Numerical simulations of hypervelocity impact of asteroid/comet on the Earth". *International Journal of Impact Engineering* 33 (2006) 713–722.
- [10] Luigi Foschini. "On the atmospheric fragmentation of small asteroids". *Astronomy & Astrophysics*. <http://arxiv.org/abs/astro-ph/0012256v2>
- [11] Victoria Garshnek, David Morrison, Frederick M. Burkle Jr.. "The mitigation, management, and survivability of asteroid/comet impact with Earth". *Space Policy* 16 (2000) 213-222.
- [12] M. H. M. Morais. "The Population of Near-Earth Asteroids in Coorbital Motion with the Earth". *Icarus* 160, 1–9 (2002) 10.1006/icar.2002.6937
- [13] B. John Garrick. "Quantifying and Controlling Catastrophic Risks". ISBN: 978-0-12-374601-6